Markerless Human Motion Tracking Using Microsoft Kinect SDK and Inverse Kinematics

Preprint · June 2019

5 authors, including:

Alireza Bilesan
Hokkaido University
5 PUBLICATIONS 8 CITATIONS

Saeed Behzadipour
Sharif University of Technology
94 PUBLICATIONS 913 CITATIONS

Teppei Tsujita
National Defense Academy of Japan
92 PUBLICATIONS 256 CITATIONS

Atsushi Konno
Hokkaido University
264 PUBLICATIONS 1,592 CITATIONS

Markerless Human Motion Tracking Using Microsoft Kinect SDK and Inverse Kinematics

Alireza Bilesan[1], Saeed Behzadipour[2], Teppei Tsujita[3], Shunsuke Komizunai[1], Atsushi Konno[1]

***Abstract*— Motion capture systems are used to gauge the kinematic features of the motion in numerous fields of research. Despite superb accuracy performance, the commercial systems are costly and difficult to use. To solve these issues, Kinect has been proposed as a low-priced markerless motion capture sensor, and its accuracy has been assessed using previous motion capture systems. However, in many of these studies, the anatomical joint angles captured using the Kinect are compared to the 3D rotation angles reported by the gold standard motion capture systems. These incompatibilities in the determination of the human joint angles can lead to higher error estimation. To accomplish a valid accuracy evaluation of the Kinect, we applied the inverse kinematics techniques in both Vicon and Kinect version 2 skeleton models to estimate lower body joint angles. The proposed method enabled us to capture the pelvic, hip, and knee joint angles using a single Kinect camera during gait. Moreover, the dependency of the proposed method to the position of the Kinect and the speed of the moving subject was investigated. In this study, the captured data of the Vicon motion capture system were used as ground-truth to assess the accuracy of the Kinect data. The results indicate the capability of Kinect in capturing human joint angles and also an affordable motion capture system applied in robotics and biomechanics applications.**

I. INTRODUCTION

Motion capture systems are utilized to reconstruct and transfer human motions into a robot. Many researchers have employed human motions in robot imitation learning and human-like motion generation [1][2][3]. For a better mimicry, human and humanoid walking patterns are compared to apply the human walking functions to the humanoid robots [4][5]. Despite high accuracy, commercial motion capture systems are costly and complicated to use. Since several cameras are required to capture one motion, the data collecting is restricted to special settings and conditions. For instance, performing multi-camera calibration is essential before each experiment. Additionally, due to the mentioned conditions, commercial systems are mainly used in indoor environments. Markerless motion capture systems were proposed to overcome the previous issues [6]. These motion analysis technologies enabled researchers

[1]Alireza Bilesan, Shunsuke Komizunai, Atsushi Konno are with the Graduate School of information Science and Technology, Hokkaido University, Kita 19 Nishi 9, Kita-ku, Sapporo, Japan bilesan@scc.ist.hokudai.ac.jp

[2]Saeed Behzadipour is with the Mechanical Engineering Department of Sharif University of Technology and Djavad Mowafaghian Research Center in Neurorehabilitation Technologies, Tehran, Iran behzadipour@sharif.edu

[3]Teppei Tsujita is with the Department of Mechanical Engineering, National Defense Academy of Japan, Yokosuka, Japan tsujita@nda.ac.jp

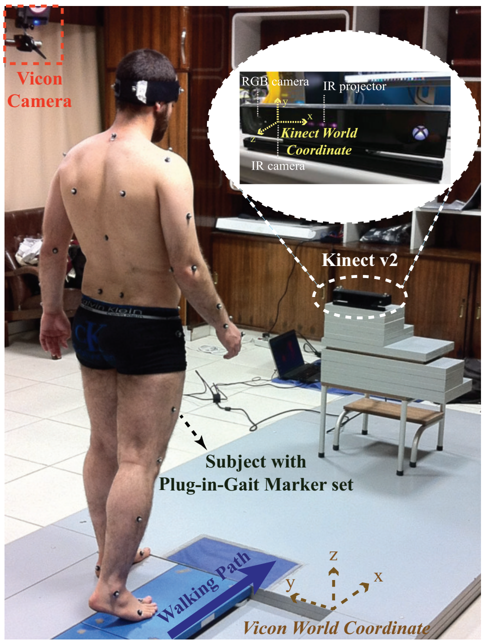

Fig. 1. Human motion tracking using Kinect v2. The Kinect accuracy is assessed using the Vicon motion capture system as the gold standard. The Kinect world coordinate is located on its IR camera, and the Vicon world coordinate is set on the floor. The plug-in-gait marker set is only used in the Vicon system in order to capture the human motion.

to evaluate movement characteristics as more cost-effective and straightforward. Despite the benefits of these new systems, systematic limitations restrain their functionality. For instance, wearable electromagnetic sensors are affected by gravity noise and signal drift [7]. Furthermore, these sensors are still costly and require a skillful data analyzer to post-process the data.

Microsoft released Kinect version 1 (Kinect v1) as an accessory for the Xbox 360 video game platform in 2010. It was designed for the gaming purposes, but it can also be utilized as a markerless, affordable, and portable motion capture sensor. The Kinect v1 consists of one IR emitter, one IR camera, and one RGB camera which acquire depth and color images of the scene. Consequently, The Depth of the scene is measured using speckle pattern technology. In 2014, Microsoft released the second version of the Kinect (Kinect v2) with enhanced RGB and IR camera resolution and wider field of view (see Fig. 1). Microsoft used a different technology called time-of-flight (TOF) in Kinect v2 in order to measure the depth of the scene [8]. The TOF technology assisted the use of the Kinect v2 in outdoor

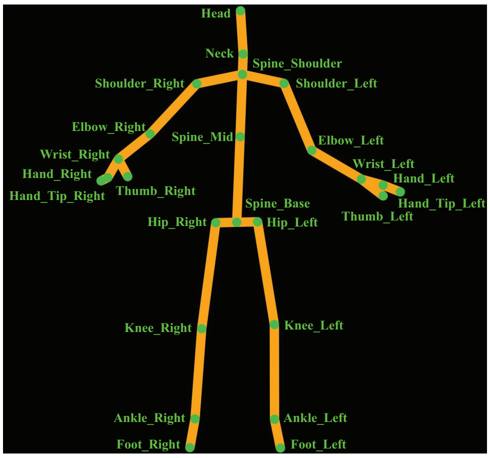

Fig. 2. Kinect v2 skeleton model with 25 estimated joints.

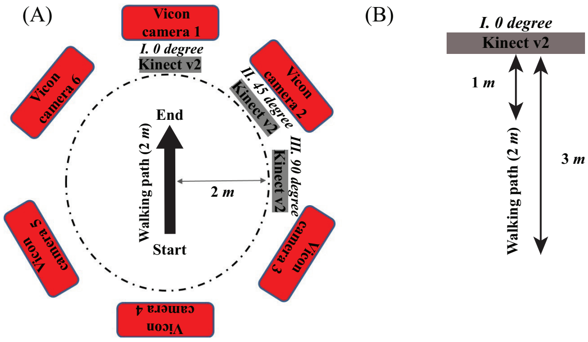

Fig. 3. Experimental setup, (A) a Kinect sensor is placed in three different positions (I. 0 degree, II. 45 degree, and III. 90 degree) to capture a walking motion. Concurrently, six Vicon motion capture cameras record the same motion. (B) walking path is located at a distance of $1\,\mathrm{m}$ to $3\,\mathrm{m}$ from the Kinect.

motion capture measurements which the speckle pattern of the Kinect v1 was proved to be remarkably affected by the sunlight. However, under direct emission of infrared light, the quality of the captured data strongly depends on the incidence angle of the rays in both versions of the Kinect [9].

With the help of the Kinect software development kit (SDK), the Kinect v2 provides a model of a three-dimensional skeleton with 25 joints of the human whose full body is placed within the field of view of the Kinect IR camera (see Fig. 2). The Kinect skeleton model has been used in various applications such as biomechanics [10], robotics [11], and computer vision [12]. Poor correlation between Kinect v1 skeleton data and commercial motion capture systems has been reported during lower extremity motion assessment in [13] and [14]. Due to the low technological specs of the Kinect v1, these deficient performances were not unforeseen. Furthermore, previous studies have shown that the Kinect is more capable of detecting spatiotemporal parameters compared to kinematic variables [15]. Thanks to the technological improvement of the Kinect v2, some researches have been able to track the sagittal plane joint angles of the human motion during functional movements [16][17][18].

Most of these studies evaluate the Kinect accuracy in capturing joint angles in the anatomical plane which is beneficial in biomechanical applications. The goal of this study is to achieve a better assessment of the Kinect spatial joint angles detection, which can be valuable in imitation learning and motion recognition applications. In addition, the relation of the Kinect accuracy with the subject position and movement speed is evaluated.

II. METHOD

A. Subjects

Five healthy adults (males, 24 years, height $175 \pm 5\,\mathrm{cm}$, weight $75 \pm 10\,\mathrm{kg}$) were selected to perform a normal gait motion at different speeds while motion capture systems were recording their movements. The subjects were asked to warm-up for five minutes before each test with different walking speeds (slow: $0.5 \pm 0.1\,\mathrm{m}/s$, moderate: $1.0 \pm 0.1\,\mathrm{m}/s$, and fast: $1.4{\pm}0.1\,\mathrm{m}/s$). Every trial was repeated 10 times for each subject, and the collected data were averaged before the statistical analysis. The motion capture systems were recording the human gait motion, simultaneously.

B. Experimental Setup

Kinematic data were captured simultaneously using a six-camera Vicon motion capture system (Vicon, Oxford, UK), sampled at 120 Hz using Vicon Nexus 2.1 software, and a Kinect v2 (Microsoft, Redmond, WA), sampled at 30 Hz using Kinect SDK 2.0. The Kinect was positioned in three different locations from the subject's walking path (0 degree: in front of the path, 45 degree: right side at a 45° angle to the path, and 90 degree: right side at a 90° angle to the path), (see Fig. 3A). Moreover, The walking path started from a distance of $3\,\mathrm{m}$ and ended at $1\,\mathrm{m}$ from the Kinect (see Fig. 3B). In order to capture full-body motion, the Kinect was located at the height of $0.75\,\mathrm{m}$ with 0.01° tilt angle (see Fig. 1).

The reflective markers were placed on each subject using the Vicon Plug-in-Gait marker set and modeled as previously described in [19]. The Subject was asked to perform a T-pose for 2 seconds to calibrate the two motion capture systems. Afterward, he started a normal walking motion through the designated path (see Fig. 1). The 3D model of the human body was created and captured in the Vicon Nexus software. Concurrently, the 3D skeleton model of the subject was generated, and the 3D positions of the body joint centers were recorded using the Kinect SDK.

C. Definition of the Joint Angles

For the hip joint angles, the Vicon software uses the Plug-in-Gait kinematic calculations to determine the hip joint angles [20]. The waist markers are used to determine an imaginary coordinate system located on the pelvis segment.

Another coordinate system is defined on the femur segment using the thigh markers and the estimated hip and knee joint centers, which are calculated using the Vicon software. [20]. Eventually, the hip joint angles are distinguished using the Euler (Cardan) angles in rotation order of YXZ (see Fig. 5). The same method used in the Plug-in-Gait model was implemented to determine the hip joint angles in the Kinect model (see Fig. 2 and Fig. 4). The Hip_Right, $Spine\_Base$, and Hip_Left joint centers are used to define a plane on the pelvis segment in the Kinect skeleton model. The vector connecting the Hip_Right to the Hip_Left is assumed as y_{pelvic} and the normal vector of the pelvic plane is defined as z_{pelvic}. subsequently, x_{pelvic} is the cross product of the two previous vectors. The same method is used to determine the left femur plane using the Hip_Left, $Knee\_Left$, and the $Ankle\_Left$ joint centers in the Kinect model. The vector connecting the $Knee\_Left$ to the Hip_Left is defined as z_{femur}, the normal vector of the femur plane is y_{femur}, and the cross product of the two previous vectors is x_{femur}. Similarly, the right femur coordinate system is defined. It is worth remarking that the $y-$axis of the coordinate systems should be directed to the left side of the body and the $z-$axis should be directed upward (see Fig. 4).

The Euler rotation angles between the world coordinate and the pelvic coordinate frames are used to determine the pelvic angles in the Vicon model (see Fig. 5). The Vicon world coordinate system is set on the floor using a Vicon calibration wand at the beginning of the calibration procedure. Furthermore, the world coordinate system of the Kinect is located on its IR camera with the demonstrated coordinate axes shown in Fig. 1 [21]. To attain the Euler angles which represent the pelvic angles, it is required to permute the world coordinate system in the Kinect environment. The coordinate axes of the permuted Kinect coordinate system are parallel to the axes of the initial Kinect world coordinate. However, the x, y, and z axes of the permuted Kinect coordinate system have changed to the new axes shown in Fig. 4, where the $x-$axis is parallel to the walking path, the $y-$axis is toward the left side of the body, and the $z-$axis is directed upward. The Euler rotation angles between the permuted Kinect coordinate and the pelvic coordinate systems indicate the pelvic angles.

Eventually, the spatial angles between the two vectors passing through the lower body links and crossed at each joint centers were used to calculate the ankle and the knee joint angles in the Kinect model (see Fig. 4). The same method was used in the Vicon model. Although these spatial angles were calculated in two different models with separate coordinate systems, we can still compare the Kinect data to the Vicon data to assess the Kinect accuracy in capturing these joint angles.

The coordinate systems definition of the body segments, in both Kinect and Vicon models, was compatible with the International Society of Biomechanics recommendations [22]. Moreover, the mathematical definitions of the joint angles in the Kinect and the Vicon model correspond as closely as possible to the existing clinical terminology.

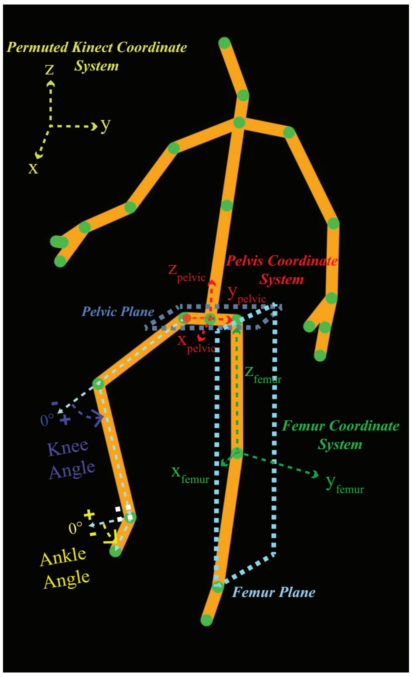

Fig. 4. Definition of the pelvic and the femur coordinate systems in the Kinect model. The hip joint angles are determined as the Euler rotation angles between the pelvic and femur coordinate systems. The pelvic angles are identified as the Euler rotation angles between the permuted Kinect coordinate and the pelvic coordinate frame. The spatial angles between the two vectors crossed at the knee and the ankle joint centers are considered as the knee and ankle joint angles, respectively.

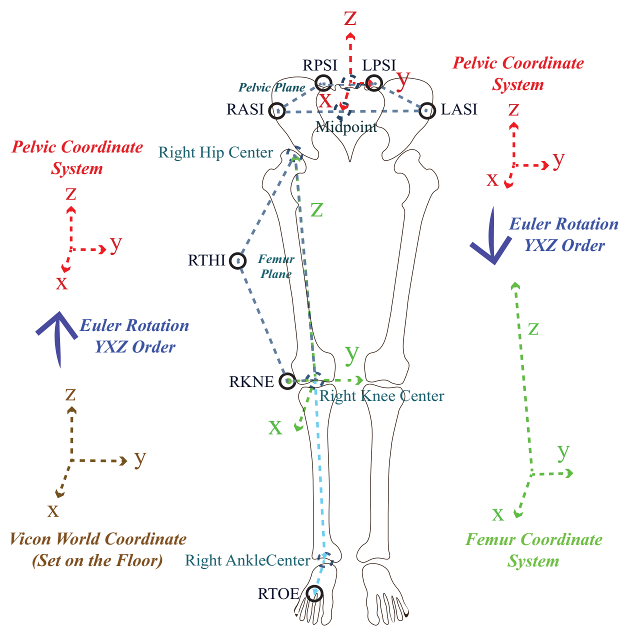

Fig. 5. Definition of the pelvic and femur coordinate systems in the Vicon model. The hip joint angles are determined as the Euler rotation angles between the pelvic and femur coordinate systems. The pelvic angles are identified as the Euler rotation angles between the Vicon world coordinate and the pelvic coordinate systems. The black solid line circles indicate the markers located on the lower body and the dashed circles indicate the estimated joint centers in the Vicon software.

D. Calculation of the Pelvic and Hip Joint Angles

To determine the hip joint angles, in both Kinect and Vicon models, the Euler (Cardan) rotation angles, which rotate the pelvic coordinate into the femur coordinate system, need to be calculated.

Equation (1) demonstrates the YXZ order Euler rotation matrix (E_{yxz}) which rotates the pelvic frame (${}^{w}F_{pelvic}$) into the femur (${}^{w}F_{femur}$) frame:

$$ {}^{w}F_{femur} = E_{yxz} \cdot^{w} F_{pelvic} \ , \qquad (1) $$

where E_{yxz} is:

$$ E_{yxz} = \begin{bmatrix} c(\psi)c(\varphi)+s(\theta)s(\psi)s(\varphi) & -c(\psi)s(\varphi)+s(\theta)s(\psi)c(\varphi) & c(\theta)s(\psi) \\ c(\theta)s(\varphi) & c(\theta)c(\varphi) & -s(\theta) \\ -s(\psi)c(\varphi)+s(\theta)c(\psi)s(\varphi) & s(\psi)s(\varphi)+s(\theta)c(\psi)c(\varphi) & c(\theta)c(\psi) \end{bmatrix} $$

the Euler matrix. Moreover, ${}^{w}F_{pelvic}$ and ${}^{w}F_{femur}$ are the projected femur and pelvic coordinate frames on the world frames. In E_{yxz}, $s(.)$ and $c(.)$ stand for $sin(.)$ and $cos(.)$, respectively. The rotation angles ψ, θ, and φ represents the rotations applied in $x-$, $y-$, and $z-$directions, respectively. Since ${}^{w}F_{pelvic}$ and ${}^{w}F_{femur}$ are orthogonal matrices, the (1) can be written as:

$$ E_{yxz} =^{w} F_{femur} \cdot^{w} F^{T}_{pelvic} = \begin{bmatrix} e_{11} & e_{12} & e_{13} \\ e_{21} & e_{22} & e_{23} \\ e_{31} & e_{32} & e_{33} \end{bmatrix} \ , \qquad (2) $$

where ${}^{w}F^{T}_{pelvic}$ is the transpose matrix of ${}^{w}F_{pelvic}$, and e_{ij} represents the elements of matrices ${}^{w}F_{femur} \cdot^{w} F^{T}_{pelvic}$. Eventually, the Euler rotation angles are attained using (2):

$$ \begin{aligned} \psi &= tan^{-1}(e_{13}/e_{33}) \\ \theta &= sin^{-1}(-e_{23}) \\ \varphi &= tan^{-1}(e_{21}/e_{22}). \end{aligned} \qquad (3) $$

These Euler rotation angles indicate the hip joint angles. ψ represents the hip flexion/extension, θ represents the hip abduction/adduction, and φ represents the hip rotation angles.

The same method is used to calculate the pelvic angles in the Kinect and Vicon models. However, The pelvic angles are calculated using the Euler rotation angles between the world and pelvic coordinate frames. As previously stated, the initial world coordinate of the Kinect requires rotations to the permuted Kinect coordinate system:

$$ {}^{w}K_{p} = \begin{bmatrix} 0 & -1 & 0 \\ 0 & 0 & 1 \\ -1 & 0 & 0 \end{bmatrix} \ , \qquad (4) $$

where ${}^{w}K_{p}$ indicates the projection of the permuted Kinect coordinate frames on the initial world frames (see Fig. 4). The pelvic joint angles are calculated using (4) as the permuted world coordinate frame in the Kinect environment. However, this rotation is not required in the Vicon environment. In pelvis, ψ represents the pelvic tilt, θ represents the pelvic obliquity, and φ represents the pelvic rotation angles.

III. RESULTS

To minimize any fluctuations in the Kinect data, a 5th-order low pass filter with a cut-off frequency of 4 Hz, was applied to the Kinect data [13]. The results of the comparison between the two motion capture systems for a single trial, when the Kinect is located in front of the path and the subject walks slowly, are shown in Fig. 6. The red-line indicates the angles captured by Vicon cameras and the black dotted line indicates the Kinect captured data for a normal gait motion. Fig. 6 illustrates the capability of the Kinect in tracking the lower body joint angles. However, there are extreme differences between the Kinect and Vicon data in the hip rotation and ankle joint angles. Even though the range of the motions in the pelvic angles are notably low, these angles and their changes could be captured appropriately.

The average RMSE error of the captured joint angles, associated with the Kinect position and the walking speed, is shown in Fig. 7. Fig. 7(A) and Fig. 7(B) indicate the relation of the RMSE error with the Kinect position, while Fig. 7(C) and Fig. 7(D) indicate the effects of the walking speed on the Kinect accuracy. The best position for the Kinect is in front of the walking path. In this case, the Kinect can estimate the skeleton of the human more precisely. Furthermore, by increasing the movement speed, the RMSE increases in the ankle and pelvic angles. However, this effect is not reflected on the knee and hip joint angles.

The average value of the joint angles correlation (μ_r), its standard deviation (SD), and the root-mean-square-error (RMSE) derived from the Kinect and Vicon data are shown in table I. The correlation coefficients and RMSE error of the pelvic rotation, hip ab/adduction, hip flex/extension, and knee flexion are within an acceptable range which indicates our method validity. However, the correlation coefficients of the pelvic obliquity, pelvic tilt, and hip rotation are considerably low, and further improvements are required in these parts. Moreover, the RMSE error in most joint angles are substantially small, and the Kinect data values are close to the Vicon data. The hip rotation angle is an internal rotation occurring over femur bone. The Kinect has extreme difficulties in estimating this joint angle. This can also be another research domain which requires further studies.

In table II, the accuracy of the proposed method in capturing human gait using Kinect v2 is compared to similar Kinect validation studies. Kharazi et al. [16] and Xu et al. [23] used Kinect v2 and v1 to capture the lower body joint angles in the sagittal plane, respectively. Importantly, Guess et al. [24] calculated the relative Cardan rotation angles of the hip and knee using the joint orientations of the Kinect SDK 2.0 model. They compared the Kinect data to the Vicon plug-in-gait model which is similar to our method. However, our method demonstrates better accuracy in capturing the hip and knee joint angles. The ankle joint angle captured in our method indicates the Kinect inability in tracking the foot segment. To overcome this problem, Bilesan et al. proposed a marker-based motion tracking using Kinect IR camera [25], which facilitated the Kinect v2 in capturing ankle joint

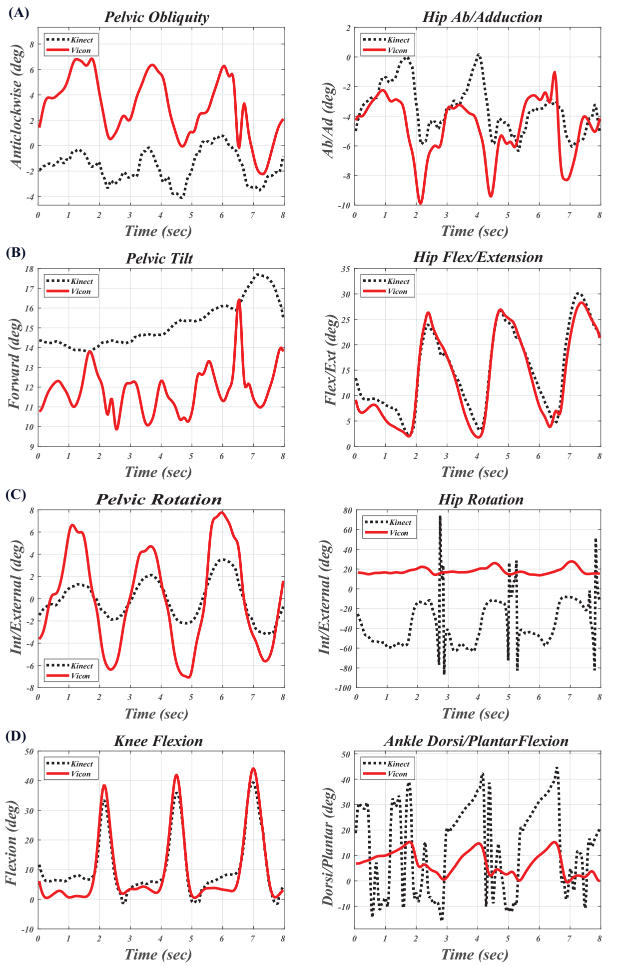

Fig. 6. Comparison of the captured joint angles using Kinect and Vicon, (A) rotation about $x-$axis (ψ), (B) rotation about $y-$axis (θ), (C) rotation about $z-$axis (φ), and (D) spatial angles. Black dotted lines: Kinect data, red solid lines: Vicon data.

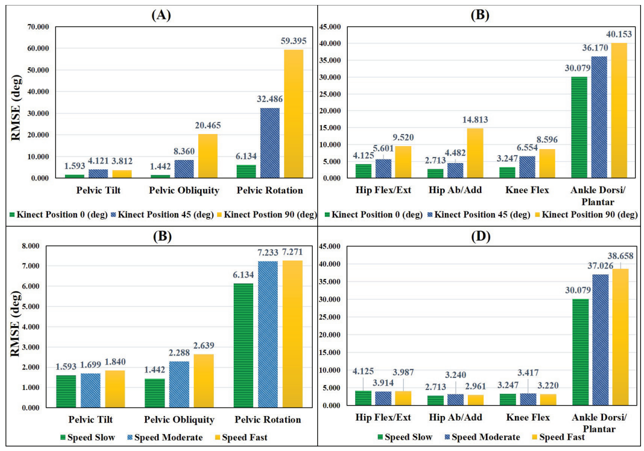

Fig. 7. RMSE of Kinect data compared to Vicon data, (A) pelvic angles measurement error related to the Kinect position, (B) lower body joint angles measurement error related to the Kinect position, (C) pelvic angles measurement error related to the motion speed, and (D) lower body joint angles measurement error related to the motion speed.

angles. The results illustrate the feasibility of the proposed motion capture system in capturing lower body joint angles using the Kinect v2.

IV. CONCLUSIONS

Capturing human joint angles using the Kinect sensor has attracted much attention with the applications in robotics, computer vision, and biomedical engineering. In this work, a markerless human motion tracking system was introduced using Kinect v2. The pelvic and hip joint angles were determined in the Kinect skeleton model using the inverse kinematics techniques. Moreover, for the knee and ankle joints, the spatial angles were determined. The same method was implemented in the skeleton model calculated in the Vicon software. Eventually, the Kinect accuracy was evaluated by comparing data obtained from the Kinect and Vicon. The mean correlation, standard deviation, and RMSE of the Kinect data were reported for the joint angles in table I, and the accuracy of our motion capture system was compared to the previous researches in table II. In order to reduce the RMSE error of the proposed motion capture system, the Kinect should be placed in front of the motion path. This indicates that the Kinect SDK have a better estimation of the human skeleton when the camera captures the hole front of the human body. Moreover, the subject would be better to perform motions with slower speed considering the Kinect low sampling time (30 Hz) (Fig. 7). The Kinect v2 is identified as a noisy sensor and its accuracy relies on its environmental situations. However, it managed to operate simultaneously with the Vicon cameras. The results illustrate the possibility of using Kinect in both human-body motion analysis and human-robot imitation tasks. However, further studies are required to improve the Kinect accuracy in estimating the ankle joint and hip rotation angles (table I).

TABLE I

MEAN CORRELATION, STANDARD DEVIATION (SD), AND RMSE ERROR BETWEEN THE MOTION CAPTURE SYSTEMS DATA IN THE MODERATE SPEED MOTION TEST. KINECT IS POSITIONED IN FRONT OF SUBJECT.

System	$\mu_r \pm$ SD	RMSE (degree)
Pelvic Obliquity	0.6641 ± 0.1204	2.288
Pelvic Tilt	0.2679 ± 0.1140	1.699
Pelvic Rotation	**0.9502 ± 0.0321**	**7.233**
Hip Ab/Adduction	**0.7562 ± 0.1739**	**3.240**
Hip Flex/Extension	**0.9779 ± 0.0113**	**3.914**
Hip Rotation	0.3592 ± 0.0663	53.996
Knee Flexion	**09834 ± 0.0314**	**3.247**
Ankle Dorsi/PlantarFlexion	0.7196 ± 0.1944	30.079

TABLE II

ERROR COMPARISON BETWEEN OUR METHOD AND PREVIOUS STUDIES.

Method	Hip_RMSE (degree)	Knee_RMSE (degree)	Ankle_RMSE (degree)
Xu et al. [23]	11.9	29.0	-
Guess et al. [24]	12	11	-
Kharazi et al. [16]	5.9	6.3	23.3
Our Method	**3.9**	**3.2**	**30.0**

As it is illustrated in Fig. 6, the Kinect data is noisy and unstable, which becomes more important in the forward dynamic simulation, where the second order differential of the joint trajectories are required. The results affirm more research is required to overcome the instability of the Kinect data to validate this sensor in robot control tasks.

REFERENCES

[1] N. S. Pollard, J. K. Hodgins, M. J. Riley, and C. G. Atkeson. Adapting human motion for the control of a humanoid robot. In IEEE International Conference on Robotics and Automation, vol. 2, pp. 1390-1397, 2002.

[2] S. Nakaoka, A. Nakazawa, F. Kanehiro, K. Kaneko, M. Morisawa, and K. Ikeuchi. Task Model of Lower Body Motion for a Biped Humanoid Robot to Imitate Human Dances. In 2005 IEEE/RSJ International Conference on Intelligent Robots and Systems, pp. 3157-3162, 2005.

[3] S. Schaal, A. Ijspeert, and A. Billard. Computational approaches to motor learning by imitation. Philosophical Transactions of the Royal Society of London. Series B: Biological Sciences, 358(1431), pp. 537-547, Feb 2003.

[4] S. Kagami, M. Mochimaru, and Y. Ehara. Measurement and Comparison of Human and Humanoid Walking. In Proceedings 2003 IEEE International Symposium on Computational Intelligence in Robotics and Automation. Computational Intelligence in Robotics and Automation for the New Millennium, vol. 2, pp. 918-922, July 2003.

[5] K. Miura, M. Morisawa, F. Kanehiro, S. Kajita, K. Kaneko, and K. Yokoi. Human-like Walking with Toe Supporting for Humanoids. In 2011 IEEE/RSJ International Conference on Intelligent Robots and Systems, pp. 4428-4435, 2011.

[6] L. Mundermann, S. Corazza, and T.P. Andriacchi. The evolution of methods for the capture of human movement leading to markerless motion capture for biomechanical applications. Journal of Neuroengineering and Rehabilitation, 3(1), p. 6, 2006.

[7] H. Luinge and P. Veltink. Measuring orientation of human body segments using miniature gyroscopes and accelerometers, Medical and Biological Engineering and computing, 43(2), pp. 273-282, 2005.

[8] J. Sell and P. O'Connor. The xbox one system on a chip and kinect sensor. IEEE Micro, 34(2), pp. 44-53, 2014.

[9] S. Zennaro. Evaluation of microsoft kinect 360 and microsoft kinect one for robotics and computer vision applications. Masters thesis, University of Padova, Italy, 2014.

[10] M. Jebeli, A. Bilesan, and A. Arshi. A study on validating kinectv2 in comparison of vicon system as a motion capture system for using in health engineering in industry. Nonlinear Engineering, 6(2), pp. 95-99, 2017.

[11] V. V. Nguyen and J. H. Lee. Full-body imitation of human motions with kinect and heterogeneous kinematic structure of humanoid robot. In 2012 IEEE/SICE International Symposium on System Integration (SII), pp. 93-98, 2012.

[12] J. Han, L. Shao, D. Xu, and J. Shotton. Enhanced computer vision with microsoft kinect sensor: A review. IEEE Transactions on Cybernetics, 43(5), pp.1318-1334, 2013.

[13] Z. Jamali and S. Behzadipour. Quantitative evaluation of parameters affecting the accuracy of microsoft kinect in gait analysis. In Proceedings of the 23rd Iranian Conference on Biomedical Engineering (ICBME), pp. 306-311, Nov 2016.

[14] A. Pfister, A.M. West, S. Bronner, and J.A. Noah. Comparative abilities of Microsoft Kinect and Vicon 3D motion capture for gait analysis. Journal of medical engineering & technology. 38(5), pp. 274-280, 2014.

[15] S. Springer and G.Y. Seligmann. Validity of the Kinect for gait assessment: a focused review. Sensors, 16(2), p.194. 2016.

[16] M. Kharazi, A. Memari, A. Shahrokhi, H. Nabavi, S. Khorami, A. Rasooli, H. Barnamei, A. Jamshidian, and M. Mirbagheri. Validity of Microsoft KinectTM for measuring gait parameters. 22nd Iranian Conference on Biomedical Engineering (ICBME), pp. 375-379 , Nov 2015.

[17] M. Eltoukhy, J. Hoon, C. Kuenze, and J. Signorile. Improved kinect-based spatiotemporal and kinematic treadmill gait assessment. Gait & Posture, 51, pp. 77-83, 2017.

[18] M. Eltoukhy, C. Kuenze, J. Oh, S. Wooten, and J.F. Signorile. kinect-based assessment of lower limb kinematics and dynamic postural control during the star excursion balance test. Gait & Posture, 58, pp. 421-427, 2017.

[19] S. Bronner. Differences in segmental coordination and postural control in a multi-joint dance movement: developpe arabesque. Journal of Dance Medicine & Science, 16(1), pp. 26-35, 2012.

[20] Plug-in gait model. http://wweb.uta.edu/faculty/ricard/classes/kine-5350/pigmanualver1.pdf. Accessed 8 November 2018.

[21] Microsoft Kinect One. $https://developer.microsoft.com/en-us/windows/kinect$. Accessed 8 November 2018.

[22] G. Wu and P.R. Cavanagh. ISB recommendations for standardization in thereporting of kinematic data. Journal of biomechanics, 28(10), pp.1257-1261, 1995.

[23] X. Xu, R. McGorry, L. Chou, J. Lin, and C. Chang. Accuracy of the Microsoft Kinect for measuring gait parameters during treadmill walking. Gait & Posture, 42(2), pp.145-151, 2015.

[24] T. Guess, S. Razu, A. Jahandar, M. Skubic, and Z. Huo. Comparison of 3D joint angles measured with the kinect 2.0 skeletal tracker versus a marker-based motion capture system. Journal of applied biomechanics, 33(2), pp. 176-181, 2017.

[25] A. Bilesan, M. Owlia, S. Behzadipour, S. Ogawa, T. Tsujita, S. Komizunai, and A. Konno. Marker-based motion tracking using Microsoft Kinect. IFAC-PapersOnLine, 51(22), pp.399-404, 2018.